



University of Groningen

Detecting chirality in two-terminal electronic devices

Yang, Xu; Wal, Caspar H. van der; Wees, van, Bart

Published in:
ArXiv

IMPORTANT NOTE: You are advised to consult the publisher's version (publisher's PDF) if you wish to cite from it. Please check the document version below.

Document Version
Early version, also known as pre-print

Publication date:
2019

[Link to publication in University of Groningen/UMCG research database](#)

Citation for published version (APA):

Yang, X., Wal, C. H. V. D., & Wees, van, B. (2019). Detecting chirality in two-terminal electronic devices. *ArXiv*.

Copyright

Other than for strictly personal use, it is not permitted to download or to forward/distribute the text or part of it without the consent of the author(s) and/or copyright holder(s), unless the work is under an open content license (like Creative Commons).

Take-down policy

If you believe that this document breaches copyright please contact us providing details, and we will remove access to the work immediately and investigate your claim.

Downloaded from the University of Groningen/UMCG research database (Pure): <http://www.rug.nl/research/portal>. For technical reasons the number of authors shown on this cover page is limited to 10 maximum.

Detecting chirality in two-terminal electronic devices

Xu Yang,^{1,*} Caspar H. van der Wal,¹ and Bart J. van Wees¹

¹*Zernike Institute for Advanced Materials, University of Groningen, NL-9747AG Groningen, The Netherlands*
(Dated: December 24, 2019)

The chirality-induced spin selectivity (CISS) effect concerns the interconversion of electronic charge and spin currents. In two-terminal (2T) devices containing a chiral (molecular) component and a ferromagnet, CISS has been detected as magnetoresistance (MR) signals, which, however, is forbidden by Onsager reciprocity in the linear response regime. Here, by unifying the description for coupled charge and spin transport in magnetic and chiral spin-charge converters, we uncover an elementary mechanism that breaks reciprocity and generates MR for nonlinear response. It requires (a) energy-dependent transport, and (b) energy relaxation in the device. The sign of the MR depends on the chirality, the charge carrier type, and the bias direction. Additionally, our formalism reveals how CISS can be detected in the linear response regime in magnet-free 2T devices, either by forming a chirality-based spin-valve using two or more chiral components, or by Hanle spin precession in devices with a single chiral component.

Chirality is discovered to induce surprisingly efficient interconversion between electronic charge and collinear spin currents, and the effect is termed chirality-induced spin selectivity (CISS) [1, 2]. It has great potential for future applications in nano-electronics and spintronics [3], and benefits chemistry by enabling an electronic method to distinguish and even separate chiral enantiomers [4]. One would naturally assume that this spin-polarizing effect can be electrically measured by connecting a ferromagnet (FM) to a chiral component (single molecule, assembly of molecules, or solid-state system) in a two-terminal (2T) geometry, such that a charge current induces a spin accumulation by flowing through the chiral component, which is subsequently detected by the FM as a charge voltage. In analogy to a conventional spin valve, this charge voltage shall change upon reversing the FM magnetization direction, producing a magnetoresistance (MR) signal. Such a (bias-dependent) MR has indeed been reported and is widely used as a proof of CISS [5–9]. However, according to Onsager reciprocity, which arises from fundamental microscopic reversibility, a 2T MR is forbidden in the linear response regime, because chirality is invariant under time reversal [10–12].

Theories have mainly focused on understanding how CISS can be generated in a chiral component [13–18], but have overlooked whether it can be detected using a 2T electronic device. The restriction imposed by reciprocity was only pointed out very recently [19, 20], and therefore it requires theories beyond the linear response regime for possible explanations of the experimentally observed 2T MR signals.

Here we uncover that a MR can arise from the breaking of Onsager reciprocity in the nonlinear regime. When the conditions for generating CISS in the chiral component are fulfilled, the emergence of the 2T MR requires two key ingredients: (a) energy-dependent electron transport due to, for instance, tunneling or thermally activated conduction through molecular orbitals; and (b) energy relaxation due to inelastic processes. Note that there exists an

interesting parallel in chemistry, which enables absolute asymmetric synthesis under the lone influence of a magnetic field or magnetization in the nonlinear regime (details see Supplementary Information A [SI.A]) [4, 21, 22].

Below, before demonstrating the emergence of MR in the nonlinear regime in 2T CISS geometries, we will first introduce a matrix formalism unifying the description of a chiral component and a FM tunnel junction/interface (FMTJ) as spin-charge converters. Afterwards, we will review several generic 2T geometries and reveal a chiral spin valve built without magnetic materials.

A UNIFIED FORMALISM FOR COUPLED CHARGE AND SPIN TRANSPORT

In the presence of spin-charge conversion, either due to time-reversal invariant spin-orbit effects such as CISS, or by breaking the time-reversal symmetry such as in a FM, the description of a generic 2T device must include not only the charge voltages as driving forces for charge and spin transport, as in the (spin-resolved) Landauer formula, but also the build-up of spin accumulations and the resulting charge and spin currents (details see SI.B) [23]. We take these into account using a transport matrix formalism.

Spin-charge conversion in a chiral component

CISS describes that a charge current through a chiral component produces collinear spin currents, as a result of spin-orbit interaction and the absence of space-inversion symmetry. Further symmetry considerations require that the sign of the spin currents must depend on the direction of the charge current and the (sign of) chirality. Note that the generation of such an effect requires a nonunitary transport mechanism inside the chiral component [24, 25], which we assume to be present

(details see SI.C). In an ideal case, as illustrated in Fig. 1, this directional, spin-dependent electron transport effectively allows only one spin orientation, say, parallel to the electron momentum, to transmit through the chiral component, and reflects and spin-flips the other [19]. The spin-flip reflection prevents a net spin current in and out of electrodes at thermodynamic equilibrium [26].

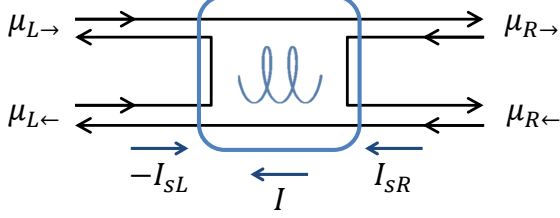


FIG. 1. Illustration of CISS (ideal case). The directional electron transmission is spin-selective, and the unfavored spin is flipped and reflected. The chiral component is indicated by the blue helix, and is assumed to favor the transmission of electrons with spin parallel to momentum. The electrons on both sides (L and R) of the chiral component are labeled with their spin-specific (\rightarrow or \leftarrow) electrochemical potentials $\mu_{L(R)\rightarrow(\leftarrow)}$. At thermodynamic equilibrium, any net charge or spin current in and out of electrodes is forbidden, but when biased, the chiral structure supports a charge current I and spin currents on both sides I_{sL} and I_{sR} . The positive currents are defined as right-to-left, i.e. when the (spin-polarized) electrons flow from left to right.

We first describe the directional electron transmission (\mathbb{T}) and reflection (\mathbb{R}) in a generalized chiral component using spin-space matrices introduced in Ref. 19. For right-moving (subscript \triangleright) electrons coming from the left-hand side of the component

$$\mathbb{T}_{\triangleright} = \begin{pmatrix} t_{\rightarrow\rightarrow} & t_{\leftarrow\rightarrow} \\ t_{\rightarrow\leftarrow} & t_{\leftarrow\leftarrow} \end{pmatrix}, \quad \mathbb{R}_{\triangleright} = \begin{pmatrix} r_{\rightarrow\rightarrow} & r_{\leftarrow\rightarrow} \\ r_{\rightarrow\leftarrow} & r_{\leftarrow\leftarrow} \end{pmatrix}, \quad (1)$$

where the matrix elements are probabilities of an electron being transmitted (t) or reflected (r) from an initial spin state (first subscript) to a final spin state (second subscript). For left-moving electrons, the corresponding matrices are the time-reversed forms of the above (details see SI.D).

We extend the above coupled charge and spin transport by converting the spin-space matrices to transport matrices that link the thermodynamic drives and responses in terms of charge and spin. We define (charge) electrochemical potential $\mu = (\mu_{\rightarrow} + \mu_{\leftarrow})/2$ and spin accumulation $\mu_s = (\mu_{\rightarrow} - \mu_{\leftarrow})/2$, as well as charge current $I = I_{\rightarrow} + I_{\leftarrow}$ and spin current $I_s = I_{\rightarrow} - I_{\leftarrow}$. A subscript R or L is added when describing the quantities on a specific side of the component. With these, for a generalized case of Fig. 1, we derive (details see SI.D)

$$\begin{pmatrix} I \\ -I_{sL} \\ I_{sR} \end{pmatrix} = -\frac{Ne}{h} \begin{pmatrix} t & s & s \\ P_r r & \gamma_r & \gamma_t \\ P_t t & \gamma_t & \gamma_r \end{pmatrix} \begin{pmatrix} \mu_L - \mu_R \\ \mu_{sL} \\ \mu_{sR} \end{pmatrix}, \quad (2)$$

where N is the number of (spin-degenerate) channels, e is elemental charge (positive value), and h is the Planck's constant. We name the 3×3 matrix the charge-spin transport matrix \mathcal{T} . All its elements are linear combinations of the spin-space \mathbb{T} and \mathbb{R} matrix elements, and represent key transport properties of the chiral component. For example, t is the (averaged) transmission probability, r is the reflection probability (note that $t+r=2$ because we have treated the two spins separately), P_t and P_r are the CISS-induced spin polarizations of the transmitted and reflected electrons, respectively. An electrochemical potential difference $\mu_L - \mu_R = -eV$ is provided by an bias voltage V .

This matrix equation fully describes the coupled charge and collinear spin transport through a (nonmagnetic) chiral component, which is subject to Onsager reciprocity in the linear response regime. This requires $\mathcal{T}_{ij}(\mathbf{H}, \mathbf{M}) = \mathcal{T}_{ji}(-\mathbf{H}, -\mathbf{M})$, where \mathbf{H} is the magnetic field and \mathbf{M} is the magnetization [10]. This then gives $P_t t = P_r r = s$. In later discussions we will connect the R -side of the chiral component to an electrode (reservoir), where $\mu_{sR} = 0$ and I_{sR} is irrelevant. The \mathcal{T} matrix then reduces to a 2×2 form (details see SI.D)

$$\begin{pmatrix} I \\ -I_{sL} \end{pmatrix} = -\frac{Ne}{h} \begin{pmatrix} t & P_t t \\ P_t t & \gamma_r \end{pmatrix} \begin{pmatrix} \mu_L - \mu_R \\ \mu_{sL} \end{pmatrix}. \quad (3)$$

Note that t and γ_r do not depend on the (sign of) chirality, while P_t changes sign when the chirality is reversed.

Spin-charge conversion in a FMTJ

To calculate the coupled charge and spin transport in a generic 2T circuit where an (achiral) ferromagnet is also present, we need to derive a similar \mathcal{T} matrix for a FMTJ. A FM breaks time-reversal symmetry and provides a spin-polarization P_{FM} to any outflowing charge current. Based on this, we obtain for the R -side of the FMTJ (details see SI.E)

$$\begin{pmatrix} I \\ I_{sR} \end{pmatrix} = -\frac{N'e}{h} \begin{pmatrix} T & -P_{FM}T \\ P_{FM}T & -T \end{pmatrix} \begin{pmatrix} \mu_L - \mu_R \\ \mu_{sR} \end{pmatrix}, \quad (4)$$

where N' is the number of (spin-degenerate) channels, and T is the electron transmission probability accounting for both spins.

The matrix \mathcal{T} here also satisfies $\mathcal{T}_{ij}(\mathbf{H}, \mathbf{M}) = \mathcal{T}_{ji}(-\mathbf{H}, -\mathbf{M})$, where a reversal of \mathbf{M} corresponds to a sign change of P_{FM} .

ORIGIN OF MR – ENERGY-DEPENDENT TRANSPORT AND ENERGY RELAXATION

No MR in the linear response regime

We model a generic 2T MR measurement geometry using Fig. 2(a). A FM and a chiral component are connected in series between two spin-unpolarized electrodes (L and R), and the difference between their electrochemical potentials $\mu_L - \mu_R = -eV$ drives charge and spin transport. We introduce a node between the FM and the chiral component, which is characterized by an electrochemical potential μ and a spin accumulation μ_s . It preserves the spin but relaxes the energy of electrons to a Fermi-Dirac distribution due to inelastic processes (e.g. electron-phonon interaction).

By adapting Eqn. 3 and Eqn. 4 in accordance with the notations in Fig. 2(a), and applying continuity condition in the node for both the charge and spin currents, we derive the 2T conductance for the linear response regime (details see SI.F)

$$G_{2T} = G_{2T} (P_{FM}^2, P_t^2), \text{ no } P_{FM}P_t \text{ term.} \quad (5)$$

It depends on the polarizations P_{FM} and P_t only to second order, and does not depend on their product $P_{FM}P_t$. Therefore, the 2T conductance remains unchanged when the sign of either P_{FM} or P_t is reversed by the reversal of either the FM magnetization direction or the chirality. This result again confirms the vanishing MR in the linear response regime, as strictly required by Onsager reciprocity [19].

This vanishing MR can be understood as a result of two simultaneous processes. First, by the conventional description, the charge current through the chiral component drives a collinear spin current and creates a spin accumulation in the node (spin injection by CISS), which is then detected as a charge voltage by the FM (spin detection by FM). This charge voltage indeed changes upon the FM magnetization reversal. However, this is always accompanied by the second process, where it is the FM that injects a spin current, and the Onsager reciprocal of CISS detects it as a charge voltage. This voltage also changes upon the FM magnetization reversal. In the linear regime, the two processes compensate each other, and the net result is a zero MR.

Emergence of MR in nonlinear regime

The key to inducing MR is to break the balance between the two processes, which can be done by using electrons at different energies for spin injection and spin detection. This requires the presence of energy relaxation inside the device, and it also needs the transport to be energy-dependent in at least one of the spin-charge

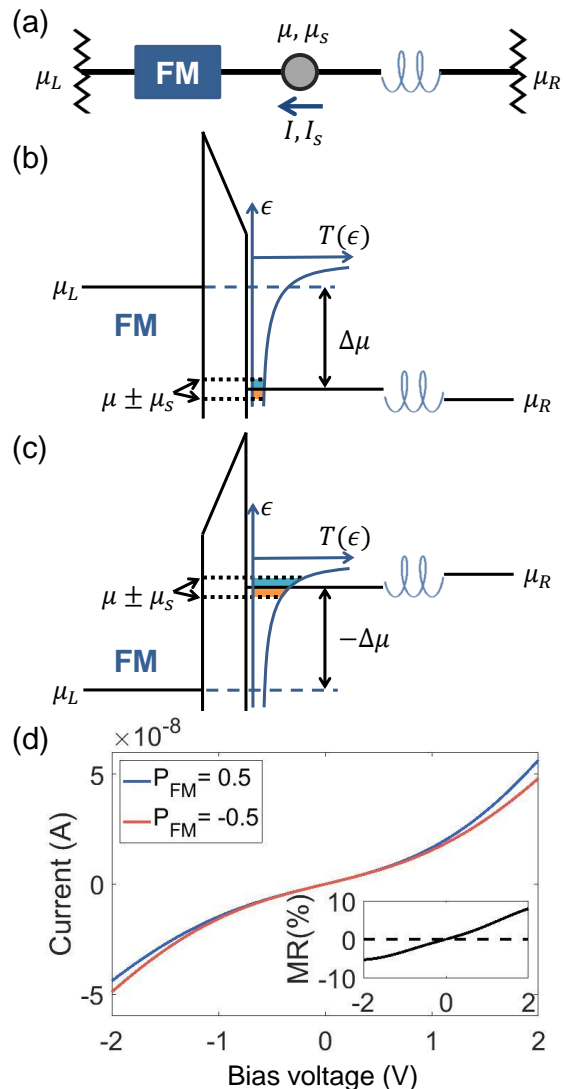


FIG. 2. Origin of MR in a generic 2T circuit. (a). A 2T circuit containing a FM and a chiral component, connected by a node. The chiral component is assumed to favor the transmission of electrons with spin parallel to momentum. (b),(c). Schematic energy diagrams of tunneling at the FMTJ under forward [(b)] and reverse [(c)] biases. The energy-dependent tunnel transmission $T(\epsilon)$ is sketched in blue, and the tunnel current affected by the spin accumulation μ_s is illustrated by the color-shaded areas (cyan and orange). (d). Example I - V curves considering the nonlinear mechanism of (b)-(c), while keeping the transmission through the chiral component constant (details see SI.G). Note that positive bias voltage corresponds to the reverse bias scenario depicted in panel (c). The MR ratio, defined as $(I_+ - I_-)/(I_+ + I_-)$, is plotted in inset. Here the subscript $+$ or $-$ denotes the corresponding sign of P_{FM} , with $P_{FM} > 0$ corresponding to a spin-right polarization for the injected electrons. The dashed line marks zero MR.

converters. Note that the energy relaxation is crucial for generating MR, because Onsager reciprocity, which holds at each energy level, would otherwise prevent a MR even in the nonlinear regime despite the energy-dependent transport. We illustrate the emergence of MR using two types of energy dependence, (a) quantum tunneling through the FMTJ, and (b) thermally activated conduction through molecular orbitals.

The asymmetric spin injection and spin detection in a FMTJ was previously discussed by Jansen et al. for a FM coupled to a semiconductor [27], and here we generalize it for our system. The energy diagrams for this tunneling process are sketched in Fig. 2(b)-(c) for opposite biases. The bias opens up an energy window $\Delta\mu = \mu_L - \mu$, and the electrons within this energy window contribute to the total charge current I . The energy distribution of the tunneling electrons follows the energy dependence of the tunnel transmission probability $T(\epsilon)$ (blue curve). Therefore, the electrons that contribute the most to the tunnel current I are those at the highest available energy, which are at μ_L in the FM under forward bias, and are at the spin-split electrochemical potentials $\mu \pm \mu_s$ in the node under reverse bias.

The spin injection process concerns the spin current I_s , which is generated by the charge current I through the FMTJ with spin polarization P_{FM} (we assume no energy dependence for P_{FM}). The total charge current consists of electrons at all available energies and is proportional to the energy integral of $T(\epsilon)$ over the entire energy window $\Delta\mu$. It is therefore symmetric for opposite biases (assuming $\mu_s \ll \Delta\mu$). In contrast, the spin detection process concerns the spin accumulation μ_s , which is only relevant to electrons at the highest energy in the node μ (Fermi level). The transmission probability at this energy, hence the detected current due to μ_s , is not symmetric for opposite biases and increases monotonically as the bias becomes more reverse. Effectively, the spin accumulation describes the deficit of one spin and the surplus of the other (as indicated by the orange- and blue-shaded areas), and therefore drives an additional charge current which is proportional to the area difference between the two color-shaded regions under the $T(\epsilon)$ curve. This area difference is not symmetric for opposite biases.

The different bias dependences for spin injection and detection break Onsager reciprocity for nonlinear response. This is also shown by the different off-diagonal terms in the nonlinear transport equation (details see SI.G)

$$\begin{pmatrix} I \\ I_s \end{pmatrix} = -\frac{N'e}{h} \begin{pmatrix} \bar{T}|_{\mu}^{\mu_L} & -P_{FM}T|_{\epsilon=\mu} \\ P_{FM}\bar{T}|_{\mu}^{\mu_L} & -T|_{\epsilon=\mu} \end{pmatrix} \begin{pmatrix} \mu_L - \mu \\ \mu_s \end{pmatrix}, \quad (6)$$

where $\bar{T}|_{\mu}^{\mu_L} = [1/(\mu_L - \mu)] \int_{\mu}^{\mu_L} T(\epsilon) d\epsilon$ is the averaged transmission over the energy window $\Delta\mu = \mu_L - \mu$, and $T|_{\epsilon=\mu}$ is the transmission evaluated at the Fermi level

of the node $\epsilon = \mu$. In the linear response regime, when $\mu_L \approx \mu$, this equation returns to Eqn. 4.

The tunnel I - V and the MR due to this mechanism are illustrated in Fig. 2(d) using realistic circuit parameters (details see SI.I). The MR ratio reaches nearly 10 % at

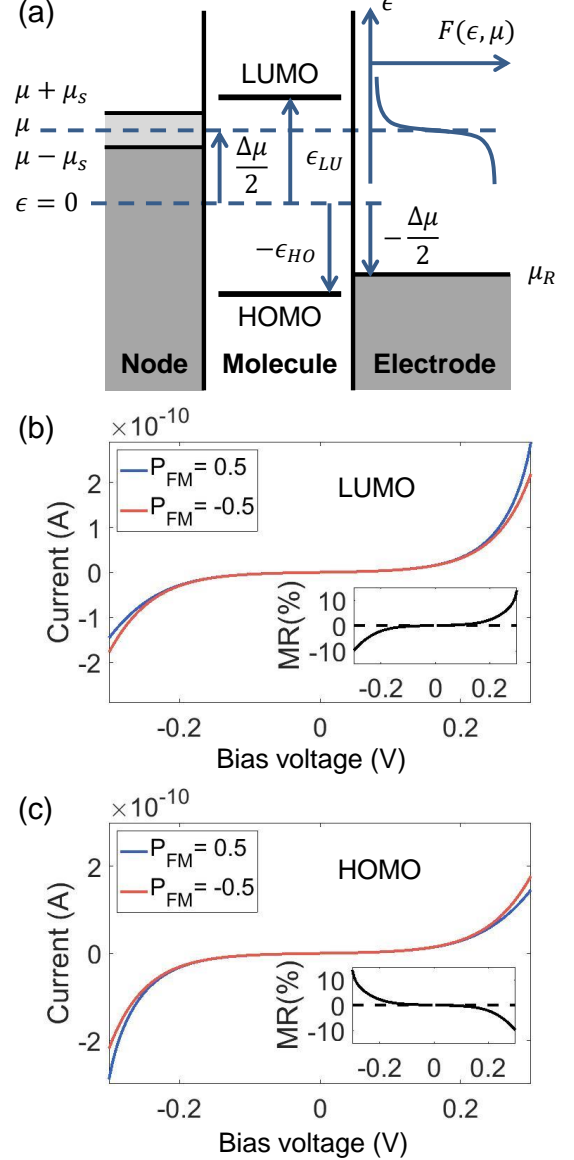


FIG. 3. Generating MR by thermally activated conduction through molecular orbitals. (a). Schematic energy diagram of resonant transmission through molecular orbitals in a chiral component (molecule). The LUMO and HOMO levels and the bias-dependent electrochemical potentials are labeled, and the energy- and bias-dependent Fermi-Dirac function $F(\epsilon, \mu)$ is sketched in blue. (b)-(c). Example I - V curves and MR (inset) due to the resonant transmission through the LUMO [(b)] and the HOMO [(c)], for the same device geometry as in Fig. 2(a) but with the transmission of the FMTJ set constant. The chiral molecule is assumed to favor the transmission of electrons with spin parallel to momentum.

large biases, but strictly vanishes at zero bias. Notably, the MR is positive under positive bias voltage (corresponds to reverse bias as in Fig. 2(c)), and it reverses sign as the bias changes sign.

The non-reciprocal spin injection and detection can also arise from the nonlinear transport through the chiral component. In principle, this could also be due to tunneling, but we focus here on another aspect, the Fermi-Dirac distribution of electrons. This is negligible when the transmission function $T(\epsilon)$ is smooth, as for the case of tunneling (thus we have assumed zero temperature for deriving Eqn. 6), but it becomes dominant when electron (or hole) transmission is only allowed at certain discrete energy levels or energy bands that are away from Fermi level, as for the case of conduction through molecular orbitals or through energy bands in semiconductors. We illustrate this in Fig. 3(a) considering the resonant transmission through the LUMO (lowest unoccupied molecular orbital) and the HOMO (highest occupied molecular orbital) of a chiral molecule (details see SI.H). For spin injection, the generated spin current is proportional to the total charge current, which depends on the electrochemical potential difference between the node and the right electrode, and is symmetric for opposite biases. In comparison, for spin detection, the spin-split electrochemical potentials in the node $\mu \pm \mu_s$ induce unequal occupations of opposite spins at each MO, depending on the MO position with respect to the node Fermi level μ , and it is not symmetric for opposite biases. This different bias dependence breaks Onsager reciprocity for nonlinear response, and gives rise to MR.

We consider the transmission through either only the LUMO or only the HOMO, and their example I - V curves and MR ratios are plotted in Fig. 3(b)-(c), respectively (details see SI.I). The MR ratio is able to reach tens of percent even at relatively small biases, and changes sign as the bias reverses. Remarkably, the bias dependence of the MR is opposite for LUMO and HOMO, implying that the nature of the charge carrier type, i.e. electrons or holes, codetermines the sign of the MR. Again, the MR strictly vanishes as the bias returns to zero (linear response regime). An overview of the signs of MR is given in SI.J.

CHIRAL SPIN VALVE

In the linear response regime, the coupled charge and spin transport at the FMTJ is described by an antisymmetric matrix (opposite off-diagonal terms), and for a chiral component the matrix is symmetric. The symmetries of these matrices are directly required by Onsager reciprocity, and have consequences when considering 2T circuits containing two generic spin-charge converting components, as illustrated in Fig. 4. As long as one of the two components is ferromagnetic (antisymmetric matrix)

and the other is not (symmetric matrix), a 2T MR signal is forbidden in the linear response regime (Fig. 4(a)). The restriction is however not in place if both matrices have the same symmetry. An example is the well-known conventional spin valve, as shown in Fig. 4(b), where two FMs are connected in series. Both FMs are described by antisymmetric matrices, and the magnetization reversal of one FM indeed changes the 2T conductance in the linear response regime.

A less obvious outcome of this symmetry consideration is that a combination of two chiral structures (both described by symmetric matrices) can also form a spin valve that operates in the linear response regime, provided that at least one of them can switch chirality, such as a molecular rotor [28]. This is illustrated in Fig. 4(c)-(d), with example I - V curves in Fig. 4(f). The geometry already produces a nonzero chirality-reversal resistance (CRR, see figure caption for definition) ratio in the linear response regime, which is further enhanced to tens of percent as the bias increases.

Finally, we introduce an experimental geometry that can directly probe the spin injection caused by a single chiral component. As shown in Fig. 4(e), the chiral component is connected to a nonmagnetic tunnel barrier via a node. Through CISS, a charge current creates a spin accumulation in the node (even in the linear response regime), which can then be suppressed using a perpendicular magnetic field due to Hanle spin precession. This results in a magnetic-field-dependent 2T conductance, and Fig. 4(g) shows the I - V curves for zero magnetic field (blue solid curve) and for when the field fully destroys the spin accumulation (black dashed curve). The corresponding MR (inset) for this geometry is nonzero in the linear response regime, and can be enhanced by increasing bias.

DISCUSSION

We have explained that energy-dependent charge transport combined with energy relaxation provide a fundamental mechanism that breaks the Onsager reciprocity in the nonlinear regime, and therefore generates a MR signal in a 2T circuit containing a ferromagnet and a chiral component. We separately discussed two sources of energy dependence, tunneling at the FMTJ and the thermally activated resonant transmission through molecular orbitals in a chiral component. In experimental conditions, the two effects can be simultaneously present. Also, the exact bias dependence may vary depending on the device details, for example, due to the presence of Schottky barriers or due to conduction through valence and conduction bands.

We have assumed that the conduction mechanisms in each separate circuit component are not changed when building them together into one device, so that the over-

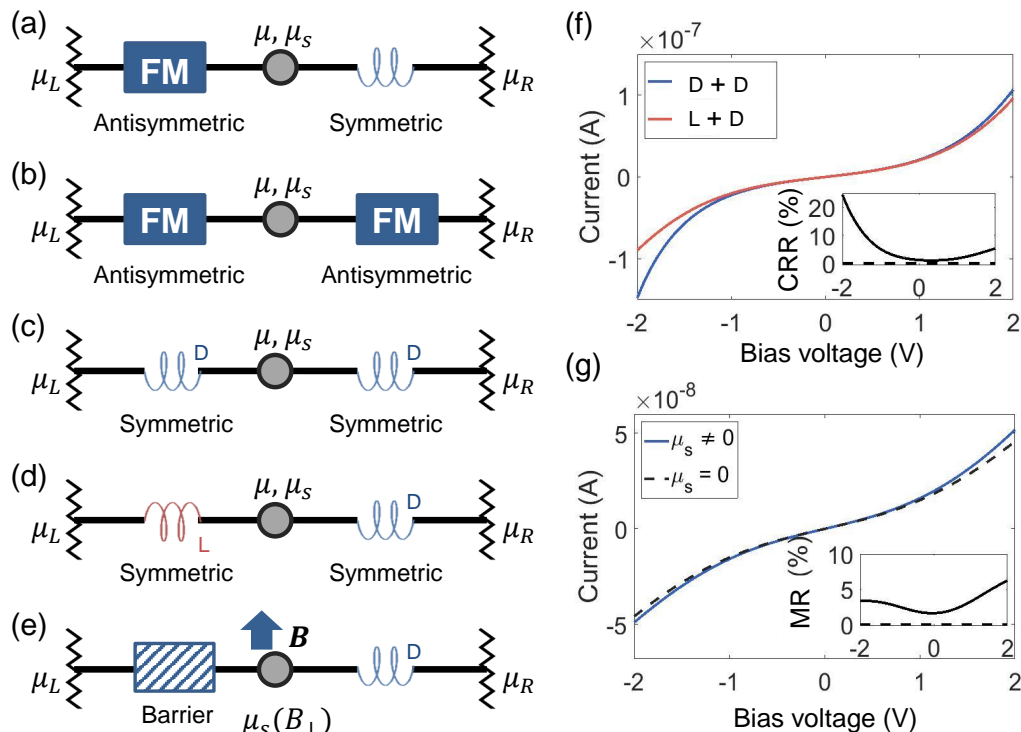


FIG. 4. Generic 2T spin-valve device geometries with the symmetry of the charge–spin transport matrix labeled for each component. (a). The aforementioned FM–chiral geometry where MR signals are strictly forbidden in the linear response regime. (b). A FM–FM geometry, as in a conventional spin valve, where MR signals are allowed in the linear regime. (c),(d). A chiral–chiral geometry for using the same [(c)] and opposite [(d)] chiralities, as marked by color and labeled with D or L (here we assume the D-chiral component favors the transmission of electrons with spin parallel to momentum, and the L-chiral component favors the anti-parallel ones), where the spin-valve effect can be achieved, even in the linear regime, by reversing the chirality of one component. (e). A geometry for directly probing the spin accumulation generated by a single chiral component. The perpendicular magnetic field B suppresses spin accumulation in the node via Hanle spin precession. (f). Example I - V curves for a chiral–chiral spin valve, with the two curves representing the geometries in panel (c) and (d) respectively. The corresponding chirality-reversal resistance (CRR) ratio, as defined by $CRR = (I_{DD} - I_{LD}) / (I_{DD} + I_{LD})$ (the two subscripts refer to the chiralities of the two chiral components), is plotted in the inset. (g). Example I - V for the geometry in panel (e), calculated for cases with μ_s either fully or not-at-all suppressed by Hanle precession. The corresponding MR is shown in inset, which is defined as the difference of the two curves divided by their sum.

all conduction is (phase) incoherent. In practice, coherent conduction mechanisms, such as direct tunneling from the FM into a MO of the chiral molecule, may also be present. Assuming fully incoherent conduction, the chirality-based spin valve geometry (Fig. 4(c-d)) resembles a conventional CPP GMR device [29], while if coherent tunneling dominates, it is comparable to a TMR device [30].

Finally, we draw attention to the sign of the nonlinear MR, which depends on the dominating nonlinear element, the bias direction, the charge carrier type, and the (sign of) chirality, as summarized in SI.J. We have plotted the MR as a function of bias while assuming the chirality and the charge carrier type remain unchanged. However, in experimental conditions, it is possible that the charge carrier type switches when the bias is reversed, and consequently the MR can have the same sign for opposite biases. Such a bias-even MR is indeed in agree-

ment with most experimental observations [5, 6, 8, 9]. The observations concerning the vanishing MR in the linear regime is however unclear, since for experiments where a linear regime can be identified, some do report a vanishing MR [8], while some do not [31]. This thus requires further investigation.

ACKNOWLEDGMENTS

This work is supported by the Zernike Institute for Advanced Materials (ZIAM), and the Spinoza prize awarded to Professor B. J. van Wees by the Nederlandse Organisatie voor Wetenschappelijk Onderzoek (NWO). The authors acknowledge discussions with R. Naaman, C. Herrmann, A. Aharony, and G.E.W. Bauer.

-
- * xu.yang@rug.nl
- [1] Ron Naaman, Yossi Paltiel, and David H Waldeck, “Chiral molecules and the electron spin,” *Nature Reviews Chemistry*, **1** (2019).
 - [2] B Göhler, V Hamelbeck, T Z Markus, M Kettner, G F Hanne, Z Vager, R Naaman, and H Zacharias, “Spin selectivity in electron transmission through self-assembled monolayers of double-stranded DNA,” *Science* **331**, 894–897 (2011).
 - [3] Igor Žutić, Jaroslav Fabian, and S Das Sarma, “Spintronics: Fundamentals and applications,” *Reviews of Modern Physics* **76**, 323 (2004).
 - [4] Koyel Banerjee-Ghosh, Oren Ben Dor, Francesco Tassinari, Eyal Capua, Shira Yochelis, Amir Capua, See-Hun Yang, Stuart SP Parkin, Soumyajit Sarkar, Leeor Kronik, *et al.*, “Separation of enantiomers by their enantiospecific interaction with achiral magnetic substrates,” *Science* **360**, 1331–1334 (2018).
 - [5] Masayuki Suda, Yuranan Thathong, Vinich Promarak, Hirotaka Kojima, Masakazu Nakamura, Takafumi Shiraogawa, Masahiro Ehara, and Hiroshi M Yamamoto, “Light-driven molecular switch for reconfigurable spin filters,” *Nature Communications* **10**, 2455 (2019).
 - [6] Haipeng Lu, Jingying Wang, Chuanxiao Xiao, Xin Pan, Xihan Chen, Roman Brunecky, Joseph J Berry, Kai Zhu, Matthew C Beard, and Zeev Vally Vardeny, “Spin-dependent charge transport through 2d chiral hybrid lead-iodide perovskites,” *Science Advances* **5**, eaay0571 (2019).
 - [7] Albert C Aragonès, Ernesto Medina, Miriam Ferrer-Huerta, Nuria Gimeno, Meritxell Teixidó, Julio L Palma, Nongjian Tao, Jesus M Ugalde, Ernest Giralt, Ismael Díez-Pérez, *et al.*, “Measuring the spin-polarization power of a single chiral molecule,” *Small* **13**, 1602519 (2017).
 - [8] Vankayala Kiran, Shinto P Mathew, Sidney R Cohen, Irene Hernández Delgado, Jérôme Lacour, and Ron Naaman, “Helicenes a new class of organic spin filter,” *Advanced Materials* **28**, 1957–1962 (2016).
 - [9] Zouti Xie, Tal Z Markus, Sidney R Cohen, Zeev Vager, Rafael Gutierrez, and Ron Naaman, “Spin specific electron conduction through DNA oligomers,” *Nano Letters* **11**, 4652–4655 (2011).
 - [10] Lars Onsager, “Reciprocal relations in irreversible processes. II.” *Physical Review* **38**, 2265 (1931).
 - [11] M Büttiker, “Symmetry of electrical conduction,” *IBM Journal of Research and Development* **32**, 317–334 (1988).
 - [12] I Adagideli, Gerrit E W Bauer, and Bertrand I Halperin, “Detection of current-induced spins by ferromagnetic contacts,” *Physical Review Letters* **97**, 256601 (2006).
 - [13] Karen Michaeli and Ron Naaman, “Origin of spin-dependent tunneling through chiral molecules,” *The Journal of Physical Chemistry C* **123**, 17043–17048 (2019).
 - [14] Ernesto Medina, Luis A González-Arraga, Daniel Finkelstein-Shapiro, Bertrand Berche, and Vladimiro Mujica, “Continuum model for chiral induced spin selectivity in helical molecules,” *The Journal of Chemical Physics* **142**, 194308 (2015).
 - [15] Ai-Min Guo and Qing-Feng Sun, “Spin-selective transport of electrons in DNA double helix,” *Physical Review Letters* **108**, 218102 (2012).
 - [16] MS Zöllner, S Varela, E Medina, V Mujica, and C Herrmann, “Chiral-induced spin selectivity: A symmetry analysis of electronic transmission,” *ChemRxiv*, 8325248.v1 (2019).
 - [17] Elena Díaz, Francisco Domínguez-Adame, Rafael Gutierrez, Gianaurelio Cuniberti, and Vladimiro Mujica, “Thermal decoherence and disorder effects on chiral-induced spin selectivity,” *The Journal of Physical Chemistry Letters* **9**, 5753–5758 (2018).
 - [18] Matthias Geyer, Rafael Gutierrez, Vladimiro Mujica, and Gianaurelio Cuniberti, “Chirality-induced spin selectivity in a coarse-grained tight-binding model for helicene,” *The Journal of Physical Chemistry C* **123**, 27230–27241 (2019).
 - [19] Xu Yang, Caspar H van der Wal, and Bart J van Wees, “Spin-dependent electron transmission model for chiral molecules in mesoscopic devices,” *Physical Review B* **99**, 024418 (2019).
 - [20] Sakse Dalum and Per Hedegård, “Theory of chiral induced spin selectivity,” *Nano Letters* **19**, 5253–5259 (2019).
 - [21] Laurence D Barron, “True and false chirality and absolute asymmetric synthesis,” *Journal of the American Chemical Society* **108**, 5539–5542 (1986).
 - [22] N Micali, H Engelkamp, P G van Rhee, P C M Christianen, L Monsù Scolaro, and J C Maan, “Selection of supramolecular chirality by application of rotational and magnetic forces,” *Nature Chemistry* **4**, 201 (2012).
 - [23] Arne Brataas, Yu V Nazarov, and Gerrit E W Bauer, “Finite-element theory of transport in ferromagnet-normal metal systems,” *Physical Review Letters* **84**, 2481 (2000).
 - [24] Jens H Bardarson, “A proof of the Kramers degeneracy of transmission eigenvalues from antisymmetry of the scattering matrix,” *Journal of Physics A: Mathematical and Theoretical* **41**, 405203 (2008).
 - [25] Shlomi Matityahu, Yasuhiro Utsumi, Amnon Aharony, Ora Entin-Wohlman, and Carlos A Balseiro, “Spin-dependent transport through a chiral molecule in the presence of spin-orbit interaction and nonunitary effects,” *Physical Review B* **93**, 075407 (2016).
 - [26] A A Kiselev and K W Kim, “Prohibition of equilibrium spin currents in multiterminal ballistic devices,” *Physical Review B* **71**, 153315 (2005).
 - [27] R Jansen, A Spiesser, H Saito, Y Fujita, S Yamada, K Hamaya, and S Yuasa, “Nonlinear electrical spin conversion in a biased ferromagnetic tunnel contact,” *Physical Review Applied* **10**, 064050 (2018).
 - [28] Nagatoshi Koumura, Robert WJ Zijlstra, Richard A van Delden, Nobuyuki Harada, and Ben L Feringa, “Light-driven monodirectional molecular rotor,” *Nature* **401**, 152 (1999).
 - [29] Mario Norberto Baibich, Jean Marc Broto, Albert Fert, F Nguyen Van Dau, Frédéric Petroff, P Etienne, G Creuzet, A Friederich, and J Chazelas, “Giant magnetoresistance of (001) fe/(001) cr magnetic superlattices,” *Physical Review Letters* **61**, 2472 (1988).
 - [30] Jagadeesh Subbaiah Moodera, Lisa R Kinder, Terrilyn M Wong, and R Meservey, “Large magnetoresistance at room temperature in ferromagnetic thin film tunnel junctions,” *Physical Review Letters* **74**, 3273 (1995).

- [31] Ramón Torres-Cavanillas, Garin Escorcía-Ariza, Prakash Chandra Mondal, Lorena E Rosaleny, Silvia Giménez-Santamarina, Isaac Brotons, Michele Sessolo, Marta Galbiati, Sergio Tatay, Alejandro Gaita-Ariño, *et al.*, “Room temperature spin filtering in chiral metalloptides,” arXiv preprint , 1905.09225 (2019).

Supplementary Information: Detecting chirality in two-terminal electronic devices

Xu Yang,^{1,*} Caspar H. van der Wal,¹ and Bart J. van Wees¹

¹*Zernike Institute for Advanced Materials, University of Groningen, NL-9747AG Groningen, The Netherlands*

(Dated: December 24, 2019)

CONTENTS

A. Comparison to absolute asymmetric (chemical) synthesis	1
B. Beyond the Landauer formula	1
C. Nonunitarity for generating CISS and inelastic processes for generating MR	1
D. Spin and charge transport in a nonmagnetic chiral component	2
E. Spin and charge transport at an achiral ferromagnetic tunnel junction/interface	4
F. Spin and charge transport in a generic 2T circuit	4
G. Reciprocity breaking by energy-dependent tunneling	5
H. Reciprocity breaking by thermally activated resonant transmission through molecular orbitals	7
I. Parameters for example I - V curves	10
J. Sign of the nonlinear 2T MR	10
References	11

A. COMPARISON TO ABSOLUTE ASYMMETRIC (CHEMICAL) SYNTHESIS

Absolute asymmetric synthesis refers to chemical reactions that yield chiral products with a net enantiomeric excess starting from achiral or racemic reactants. Generally, it requires the presence of a truly chiral external influence, which, according to Barron [S1], is a physical quantity that can appear in two degenerate forms (e.g. opposite signs of one physical quantity, or parallel and anti-parallel alignments of two vectors), which are interconverted by space-inversion but not time-reversal. Following this, the lone influence of a magnetic field, which reverses sign under time-reversal but not space-inversion, is not truly chiral, and therefore should not induce absolute asymmetric synthesis.

Just like Onsager reciprocity, this true-chirality consideration is based on microscopic reversibility, and therefore is only strict in the linear response regime (in the vicinity of thermodynamic equilibrium). Barron later pointed out that [S2], in a chemical reaction that would yield a racemic mixture (of enantiomers), the presence of a magnetic field allows different reaction rates toward opposite enantiomers. This creates an enantiomeric excess away from equilibrium, which should eventually disappear as the system returns to equilibrium. However, if the nonequilibrium enantiomeric excess is amplified, for example by self-assembly or crystallization, absolute asymmetric synthesis is induced, and this was later demonstrated experimentally [S3, S4].

This shows that a time-reversal-breaking influence (the magnetic field), albeit not being truly chiral, can distinguish and separate enantiomers away from thermodynamic equilibrium. By the same token, in the 2T circuit we discuss, the FM breaks time reversal symmetry and can therefore indeed distinguish enantiomers away from equilibrium, i.e. in the nonlinear regime. Therefore, the nonlinear conductance of the 2T circuit may depend on the chirality of the circuit component, as well as the magnetization direction of the FM.

B. BEYOND THE LANDAUER FORMULA

The Landauer formula describes the electrical conductance of a conductor using its scattering properties. Particularly, it expresses conductance in terms of transmission probabilities between electrodes, but does not require the use of reflection probabilities. Moreover, it considers that the charge (and spin) transport are solely driven by a charge bias, and neglects possible spin accumulations in the circuit. For a 2T device, it allows two independent parameters (charge and spin transmission probability) for the description of coupled charge and spin transport.

We point out here that, a full description of the coupled charge and spin transport must extend beyond the conventional spin-resolved Landauer formula, and include also the (spin-flip) reflection terms and the build-up of spin accumulations, which also act as driving forces of the transport. This point was also earlier raised for a FM-normal metal system [S5]. Following this, we need to characterize the (twofold rotationally symmetric) chiral component using four independent parameters, see the matrix in Eqn. S13, contrasting to the two parameters mentioned earlier.

C. NONUNITARITY FOR GENERATING CISS AND INELASTIC PROCESSES FOR GENERATING MR

The generation of CISS requires the presence of nonunitary effects inside the chiral component, because the Kramers' degeneracy would otherwise require equal transmission probabilities for opposite spin orientations [S6, S7]. These nonunitary effects break the phase information of a transmitting electron, but does not necessarily alter its energy.

The presence of these nonunitary effects only allows the generation of CISS, but does not guarantee the generation of a 2T MR. These nonunitary effects do not (necessarily) break the Onsager reciprocity, and therefore a 2T MR is still forbidden in the linear response regime. Even when considering energy-dependent transport in the nonlinear regime ($|eV| > k_B T$), since at each energy level the Onsager reciprocity still holds, a 2T MR cannot arise.

The emergence of MR, as we discussed, requires energy relaxation in the device. These relaxation processes not only break the phase information, but also alter the energy of the electrons, and rearrange them according to Fermi-Dirac distribution. We have assumed that they do not change the spin orientation of the electrons. In principle, we can also include spin relaxation in the node, which we expect to reduce the MR without changing its sign.

D. SPIN AND CHARGE TRANSPORT IN A NONMAGNETIC CHIRAL COMPONENT

In the main text we introduced the spin-space transmission and reflection matrices for the right-moving electrons in a (nonmagnetic) chiral component (Eqn. ??)

$$\mathbb{T}_{\triangleright} = \begin{pmatrix} t_{\rightarrow\rightarrow} & t_{\leftarrow\rightarrow} \\ t_{\rightarrow\leftarrow} & t_{\leftarrow\leftarrow} \end{pmatrix}, \quad \mathbb{R}_{\triangleright} = \begin{pmatrix} r_{\rightarrow\rightarrow} & r_{\leftarrow\rightarrow} \\ r_{\rightarrow\leftarrow} & r_{\leftarrow\leftarrow} \end{pmatrix}. \quad (\text{S1})$$

For the left-moving electrons, the matrices are the time-reversed form of the above

$$\mathbb{T}_{\triangleleft} = \begin{pmatrix} t_{\leftarrow\leftarrow} & t_{\rightarrow\leftarrow} \\ t_{\leftarrow\rightarrow} & t_{\rightarrow\rightarrow} \end{pmatrix}, \quad \mathbb{R}_{\triangleleft} = \begin{pmatrix} r_{\leftarrow\leftarrow} & r_{\rightarrow\leftarrow} \\ r_{\leftarrow\rightarrow} & r_{\rightarrow\rightarrow} \end{pmatrix}. \quad (\text{S2})$$

Note that these matrices are not suitable for describing magnetic components where time-reversal symmetry is not preserved, and we have assumed the chiral component is symmetric (i.e. a twofold rotational symmetry with axis perpendicular to the electron pathway, this ensures that for oppositely moving electrons, the spin polarization only changes sign).

We use spin-space column vector to describe electrochemical potentials and currents on both sides of the molecule, and following Ref. S8 we have

$$\begin{pmatrix} I_{L\rightarrow} \\ I_{L\leftarrow} \end{pmatrix} = -\frac{Ne}{h} \left[(\mathbb{I} - \mathbb{R}_{\triangleright}) \begin{pmatrix} \mu_{L\rightarrow} \\ \mu_{L\leftarrow} \end{pmatrix} - \mathbb{T}_{\triangleleft} \begin{pmatrix} \mu_{R\rightarrow} \\ \mu_{R\leftarrow} \end{pmatrix} \right], \quad (\text{S3a})$$

$$-\begin{pmatrix} I_{R\rightarrow} \\ I_{R\leftarrow} \end{pmatrix} = -\frac{Ne}{h} \left[(\mathbb{I} - \mathbb{R}_{\triangleleft}) \begin{pmatrix} \mu_{R\rightarrow} \\ \mu_{R\leftarrow} \end{pmatrix} - \mathbb{T}_{\triangleright} \begin{pmatrix} \mu_{L\rightarrow} \\ \mu_{L\leftarrow} \end{pmatrix} \right], \quad (\text{S3b})$$

where N is the number of spin-degenerate channels.

We define charge electrochemical potential $\mu = (\mu_{\rightarrow} + \mu_{\leftarrow})/2$ and spin accumulation $\mu_s = (\mu_{\rightarrow} - \mu_{\leftarrow})/2$, as well as charge current $I = I_{\rightarrow} + I_{\leftarrow}$ and spin current $I_s = I_{\rightarrow} - I_{\leftarrow}$. We will describe both charge and spin in electrical units.

Following these definitions, we have

$$I = I_{L\rightarrow} + I_{L\leftarrow} = I_{R\rightarrow} + I_{R\leftarrow}, \quad (\text{S4a})$$

$$I_{sL} = I_{L\rightarrow} - I_{L\leftarrow}, \quad (\text{S4b})$$

$$I_{sR} = I_{R\rightarrow} - I_{R\leftarrow}, \quad (\text{S4c})$$

$$\mu_L = (\mu_{L\rightarrow} + \mu_{L\leftarrow})/2, \quad (\text{S4d})$$

$$\mu_R = (\mu_{R\rightarrow} + \mu_{R\leftarrow})/2, \quad (\text{S4e})$$

$$\mu_{sL} = (\mu_{L\rightarrow} - \mu_{L\leftarrow})/2, \quad (\text{S4f})$$

$$\mu_{sR} = (\mu_{R\rightarrow} - \mu_{R\leftarrow})/2. \quad (\text{S4g})$$

Combining Eqn. S3 and Eqn. S4, we can derive

$$\begin{pmatrix} I \\ -I_{sL} \\ I_{sR} \end{pmatrix} = -\frac{Ne}{h} \begin{pmatrix} t & s & s \\ P_r r & \gamma_r & \gamma_t \\ P_t t & \gamma_t & \gamma_r \end{pmatrix} \begin{pmatrix} \mu_L - \mu_R \\ \mu_{sL} \\ \mu_{sR} \end{pmatrix}, \quad (\text{S5})$$

which is Eqn. ?? in the main text, and $\mu_L - \mu_R = -eV$ is induced by a bias voltage V . The matrix elements are

$$t = t_{\rightarrow\rightarrow} + t_{\rightarrow\leftarrow} + t_{\leftarrow\rightarrow} + t_{\leftarrow\leftarrow}, \quad (\text{S6a})$$

$$r = r_{\rightarrow\rightarrow} + r_{\rightarrow\leftarrow} + r_{\leftarrow\rightarrow} + r_{\leftarrow\leftarrow} = 2 - t, \quad (\text{S6b})$$

$$\gamma_t = t_{\rightarrow\rightarrow} - t_{\rightarrow\leftarrow} - t_{\leftarrow\rightarrow} + t_{\leftarrow\leftarrow}, \quad (\text{S6c})$$

$$\gamma_r = r_{\rightarrow\rightarrow} - r_{\rightarrow\leftarrow} - r_{\leftarrow\rightarrow} + r_{\leftarrow\leftarrow} - 2, \quad (\text{S6d})$$

$$P_t = (t_{\rightarrow\rightarrow} - t_{\rightarrow\leftarrow} + t_{\leftarrow\rightarrow} - t_{\leftarrow\leftarrow})/t, \quad (\text{S6e})$$

$$P_r = (r_{\rightarrow\rightarrow} - r_{\rightarrow\leftarrow} + r_{\leftarrow\rightarrow} - r_{\leftarrow\leftarrow})/r, \quad (\text{S6f})$$

$$s = t_{\rightarrow\rightarrow} + t_{\rightarrow\leftarrow} - t_{\leftarrow\rightarrow} - t_{\leftarrow\leftarrow} \quad (\text{S6g})$$

$$= -r_{\rightarrow\rightarrow} - r_{\rightarrow\leftarrow} + r_{\leftarrow\rightarrow} + r_{\leftarrow\leftarrow}. \quad (\text{S6h})$$

For $r = 2 - t$ and the two expressions of s , we have used the condition of charge conservation

$$t_{\rightarrow\rightarrow} + t_{\rightarrow\leftarrow} + r_{\rightarrow\rightarrow} + r_{\rightarrow\leftarrow} = 1, \quad (\text{S7a})$$

$$t_{\leftarrow\rightarrow} + t_{\leftarrow\leftarrow} + r_{\leftarrow\rightarrow} + r_{\leftarrow\leftarrow} = 1. \quad (\text{S7b})$$

Among the above matrix elements, P_t , P_r , and s change sign when the chirality is reversed. For achiral components where there is no spin selective transport, we have $P_t = P_r = s = 0$, and the transport matrix is symmetric.

Note that in Eqn. ?? we have defined the vector of currents (thermodynamic response) using $-I_{sL}$ and I_{sR} , so that the transport matrix is symmetric in the linear response regime. Following this, as shown in Fig. ??, the chiral component acts as a source (or sink) of spin currents when biased.

We can rewrite γ_t and γ_r as transmission-dependent quantities

$$\gamma_r = r - (P_r r + s)/\eta_r - 2 = -t - (P_r r + s)/\eta_r, \quad (\text{S8a})$$

$$\gamma_t = -t + (P_t t + s)/\eta_t, \quad (\text{S8b})$$

where

$$\eta_r = \frac{r_{\leftarrow\rightarrow} - r_{\rightarrow\leftarrow}}{r_{\leftarrow\rightarrow} + r_{\rightarrow\leftarrow}}, \quad (\text{S9a})$$

$$\eta_t = \frac{t_{\rightarrow\rightarrow} - t_{\leftarrow\leftarrow}}{t_{\rightarrow\rightarrow} + t_{\leftarrow\leftarrow}}, \quad (\text{S9b})$$

are quantities between ± 1 and change sign under chirality reversal.

Next, for chiral components where P_t , P_r , and s are nonzero, the Onsager reciprocity requires the 3×3 matrix to be symmetric [S9], which gives

$$P_t t = P_r r = s, \quad (\text{S10})$$

and therefore

$$t_{\rightarrow\leftarrow} = t_{\leftarrow\rightarrow}, \quad (\text{S11a})$$

$$r_{\rightarrow\rightarrow} = r_{\leftarrow\leftarrow}, \quad (\text{S11b})$$

$$t_{\rightarrow\rightarrow} - t_{\leftarrow\leftarrow} = r_{\leftarrow\rightarrow} - r_{\rightarrow\leftarrow}. \quad (\text{S11c})$$

These expressions show that, for any finite P_t (spin polarization of transmitted electrons), P_r (spin polarization of reflected electrons) must also be nonzero, which then requires the presence of spin-flip reflections [S8]. This is again in agreement with the fundamental considerations based on zero charge and spin currents in electrodes at equilibrium.

Further, we obtain

$$\gamma_r = -(1 + 2P_t/\eta_r)t, \quad (\text{S12a})$$

$$\gamma_t = -(1 - 2P_t/\eta_t)t. \quad (\text{S12b})$$

which allows us to rewrite the transport matrix equation in terms of t

$$\begin{pmatrix} I \\ -I_{sL} \\ I_{sR} \end{pmatrix} = -\frac{Ne}{h} \begin{pmatrix} t & P_t t & P_t t \\ P_t t & -(1 + 2P_t/\eta_r)t & -(1 - 2P_t/\eta_t)t \\ P_t t & -(1 - 2P_t/\eta_t)t & -(1 + 2P_t/\eta_r)t \end{pmatrix} \begin{pmatrix} \mu_L - \mu_R \\ \mu_{sL} \\ \mu_{sR} \end{pmatrix}. \quad (\text{S13})$$

Note that P_t , η_t , and η_r all change sign when the chirality is reversed, and t , P_t/η_t , and P_t/η_r are always positive.

In later discussions we connect the right-hand side of the nonmagnetic component to an electrode (see Fig. ??(a)) where the spin accumulation μ_{sR} is zero and the spin current I_{sR} is irrelevant. This reduces the matrix equation to

$$\begin{pmatrix} I \\ -I_{sL} \end{pmatrix} = -\frac{Ne}{h} \begin{pmatrix} t & P_t t \\ P_t t & -(1 + 2P_t/\eta_r)t \end{pmatrix} \begin{pmatrix} \mu_L - \mu_R \\ \mu_{sL} \end{pmatrix}, \quad (\text{S14})$$

which is equivalent to Eqn. ??.

E. SPIN AND CHARGE TRANSPORT AT AN ACHIRAL FERROMAGNETIC TUNNEL JUNCTION/INTERFACE

In a FM, time-reversal symmetry is broken and the Kramers degeneracy is lifted. The FMTJ provides a spin polarization to any current that flows through, and reciprocally, it generates a charge voltage upon a spin accumulation at its interface. In terms of spin and charge transport, the FMTJ allows different conductances for electrons with opposite spins, and the difference depends on the spin polarization P_{FM} . Inside the FM spin relaxation is strong and the spin accumulation is considered zero. For our discussions, the FM is always connected to the left of the node, we thus only consider the R interface of the FM with a spin accumulation μ_{sR} . Following the discussion provided in Ref. S10, the spin-specific currents on the R -side are therefore

$$I_{\rightarrow} = -\frac{1}{e}G_{\rightarrow}[\mu_L - (\mu_R + \mu_{sR})], \quad (\text{S15a})$$

$$I_{\leftarrow} = -\frac{1}{e}G_{\leftarrow}[\mu_L - (\mu_R - \mu_{sR})], \quad (\text{S15b})$$

where $G_{\rightarrow(\leftarrow)}$ is the spin-specific tunnel conductance. We define the total conductance $G_{FM} = G_{\rightarrow} + G_{\leftarrow}$ and FM spin-polarization $P_{FM} = (G_{\rightarrow} - G_{\leftarrow})/(G_{\rightarrow} + G_{\leftarrow})$. We also introduce a transmission coefficient T ($0 \leq T \leq 2$) to distinguish G_{FM} from ideal transmission. The charge and spin currents on the R interface of the FM can thus be written as

$$\begin{pmatrix} I \\ I_{sR} \end{pmatrix} = -\frac{N'e}{h} \begin{pmatrix} T & -P_{FM}T \\ P_{FM}T & -T \end{pmatrix} \begin{pmatrix} \mu_L - \mu_R \\ \mu_{sR} \end{pmatrix}, \quad (\text{S16})$$

where N' is the number of spin-degenerate channels in the FMTJ.

This matrix gives the spin and charge response of the FMTJ, and unlike for a chiral molecule, this matrix fulfills the Onsager reciprocity by being antisymmetric (opposite off-diagonal terms), because upon magnetic field and magnetization reversal, the FM spin polarization P_{FM} changes sign [S9].

F. SPIN AND CHARGE TRANSPORT IN A GENERIC 2T CIRCUIT

We consider a generic 2T circuit like the one shown in Fig. ??(a). Our goal here is to derive the quantities I , μ , and μ_s as a function of 2T bias $\mu_L - \mu_R$. We rewrite the transport matrices into conductance matrices, and obtain for the left and right side of the node

$$\begin{pmatrix} I \\ I_s \end{pmatrix} = -\frac{1}{e} \begin{pmatrix} G_1 & G_2 \\ G_3 & G_4 \end{pmatrix} \begin{pmatrix} \mu_L - \mu \\ \mu_s \end{pmatrix}, \quad (\text{S17a})$$

$$\begin{pmatrix} I \\ -I_s \end{pmatrix} = -\frac{1}{e} \begin{pmatrix} g_1 & g_2 \\ g_3 & g_4 \end{pmatrix} \begin{pmatrix} \mu - \mu_R \\ \mu_s \end{pmatrix}. \quad (\text{S17b})$$

At steady state the continuity condition requires the currents I and I_s are equal for both equations. This condition allows us to derive

$$\begin{aligned} \mu &= \mu_R + \frac{G_3(G_2 - g_2) - G_1(G_4 + g_4)}{f} (\mu_L - \mu_R) \\ &= \mu_L - \frac{g_3(g_2 - G_2) - g_1(G_4 + g_4)}{f} (\mu_L - \mu_R), \end{aligned} \quad (\text{S18a})$$

$$\mu_s = \frac{(G_3/G_1 + g_3/g_1)G_1g_1}{f} (\mu_L - \mu_R), \quad (\text{S18b})$$

$$I = \frac{G_1g_2g_3 + g_1G_2G_3 - G_1g_1(G_4 + g_4)}{f} (\mu_L - \mu_R), \quad (\text{S18c})$$

where the coefficient f is

$$f = (G_3 - g_3)(G_2 - g_2) - (G_1 + g_1)(G_4 + g_4). \quad (\text{S19})$$

Notably, f depends on $(G_3 - g_3)(G_2 - g_2)$, and for our linear-regime example using a FM with $G_2 = -G_3$ and a chiral component with $g_2 = g_3$, f only depends on $g_3^2 - G_3^2$, which does not change when either the FM magnetization or the

chirality is reversed. Moreover, the charge current I only depends on g_3^2 and G_3^2 , and therefore remains unchanged under magnetization or chirality reversal. In contrast, the spin accumulation μ_s depends on G_3 and g_3 , and the charge distribution indicated by μ depends on G_3g_2 or g_3G_2 . Both μ_s and μ therefore indeed change upon magnetization or chirality reversal, and can be detected using three-terminal or four-terminal measurement.

If the two circuit components would both be FM (antisymmetric G and g matrices) or both be chiral (symmetric G and g matrices), then the coefficient f contains the cross products G_3g_2 and G_2g_3 , and therefore gives rise to a 2T current that does change upon magnetization or chirality reversal.

G. RECIPROCITY BREAKING BY ENERGY-DEPENDENT TUNNELING

Here we derive the energy dependence of the charge and spin tunneling through the FM interface following the discussion of Jansen et al. [S10], and derive the subsequent nonlinear coupled charge and spin transport equations.

Consider a biased symmetric rectangular tunnel barrier with height Φ and width w between the FM and the node, as shown in Fig. S1. The reference energy $\epsilon = 0$ is chosen as the average of μ_L and μ , so that the average barrier height does not change with bias. The bias voltage $V = -\Delta\mu/e$ is applied, so that $\mu_L = \Delta\mu/2$, $\mu = -\Delta\mu/2$, $\mu_{\rightarrow} = -\Delta\mu/2 + \mu_s$, and $\mu_{\leftarrow} = -\Delta\mu/2 - \mu_s$. For simplicity, we assume the barrier height (evaluated at the center of the tunnel barrier) is constant, the tunneling is one dimensional, and the electrostatic potential drop across the tunnel barrier is exactly $-eV$.

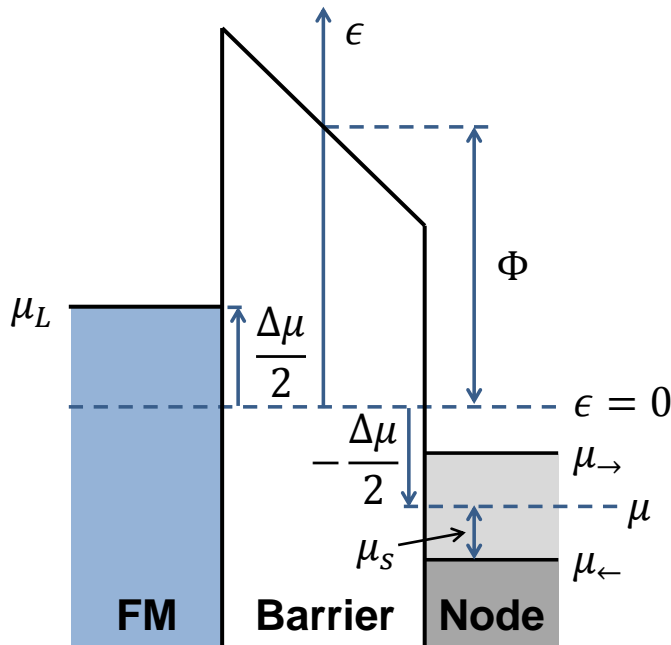


FIG. S1. Energy diagram of the tunnel barrier at the ferromagnet interface. Details see text.

The energy-dependent electron transmission function is

$$T(\epsilon) = 2 \exp\left(-\beta (\Phi - \epsilon)^{1/2}\right), \quad (\text{S20})$$

where $\beta = 2w\sqrt{2m/\hbar^2}$, with m being the (effective) electron mass and \hbar the reduced Planck's constant.

The total transmitted current is an energy-integral of two energy-dependent functions: (1) the transmission function $T(\epsilon)$, and (2) the voltage-dependent Fermi-Dirac distribution functions in both electrodes. The two parts dominate at different bias regimes with respect to the thermal activation energy $k_B T$, where k_B is the Boltzmann constant and T is temperature. For tunneling, typically we have $|eV| \gg k_B T$, and therefore we assume zero temperature for convenience. The Fermi-Dirac distribution functions then become Heaviside step functions with the step at μ_L for the left electrode and at μ_{\rightarrow} and μ_{\leftarrow} for the two spin species in the node.

Assuming P_{FM} does not depend on energy, the energy-integrated tunnel current for each spin species through the FMTJ is

$$I_{\rightarrow}(\Delta\mu, \mu_s) = -\frac{N'e}{h} \frac{1 + P_{FM}}{2} \int_{\mu_{\rightarrow}}^{\mu_L} T(\epsilon) d\epsilon, \quad (\text{S21a})$$

$$I_{\leftarrow}(\Delta\mu, \mu_s) = -\frac{N'e}{h} \frac{1 - P_{FM}}{2} \int_{\mu_{\leftarrow}}^{\mu_L} T(\epsilon) d\epsilon. \quad (\text{S21b})$$

The range of the integrals can be rewritten as

$$\text{for } I_{\rightarrow} : \int_{\mu_{\rightarrow}}^{\mu_L} d\epsilon = \int_{\mu}^{\mu_L} d\epsilon - \int_{\mu}^{\mu_{\rightarrow}} d\epsilon, \quad (\text{S22a})$$

$$\text{for } I_{\leftarrow} : \int_{\mu_{\leftarrow}}^{\mu_L} d\epsilon = \int_{\mu}^{\mu_L} d\epsilon + \int_{\mu_{\leftarrow}}^{\mu} d\epsilon. \quad (\text{S22b})$$

We denote the two integrals on the right-hand side of the expressions $I_{\rightarrow(\leftarrow)}^{(1)}$ and $I_{\rightarrow(\leftarrow)}^{(2)}$ respectively, so that we have $I_{\rightarrow} = I_{\rightarrow}^{(1)} + I_{\rightarrow}^{(2)}$ and $I_{\leftarrow} = I_{\leftarrow}^{(1)} + I_{\leftarrow}^{(2)}$. The first integral $I_{\rightarrow(\leftarrow)}^{(1)}$ depends on the electrochemical potential difference across the barrier, $\Delta\mu$, and thus describes the bias-induced transport. In contrast, the second integral $I_{\rightarrow(\leftarrow)}^{(2)}$ depends on μ and μ_s in the node, and it vanishes when $\mu_s = 0$, and therefore it describes the spin-accumulation-induced correction to the first integral. We will treat the two integrals separately.

The bias-induced charge and spin currents are

$$\begin{aligned} I^{(1)} &= I_{\rightarrow}^{(1)} + I_{\leftarrow}^{(1)} \\ &= -\frac{N'e}{h} \int_{\mu}^{\mu_L} T(\epsilon) d\epsilon \\ &= -\frac{N'e}{h} (\bar{T}|_{\mu}^{\mu_L}) \Delta\mu, \end{aligned} \quad (\text{S23a})$$

$$\begin{aligned} I_s^{(1)} &= I_{\rightarrow}^{(1)} - I_{\leftarrow}^{(1)} \\ &= -\frac{N'e}{h} P_{FM} \int_{\mu}^{\mu_L} T(\epsilon) d\epsilon \\ &= -\frac{N'e}{h} (P_{FM} \bar{T}|_{\mu}^{\mu_L}) \Delta\mu, \end{aligned} \quad (\text{S23b})$$

where the averaged transmission within the bias window is defined as

$$\bar{T}|_{\mu}^{\mu_L} = \frac{1}{\Delta\mu} \int_{\mu}^{\mu_L} T(\epsilon) d\epsilon. \quad (\text{S24})$$

Note that when $\Delta\mu$ changes sign, the integral changes sign too, and therefore $\bar{T}|_{\mu}^{\mu_L}$ is an even function of $\Delta\mu$.

For the spin-accumulation-induced currents, we have

$$\begin{aligned} I^{(2)} &= I_{\rightarrow}^{(2)} + I_{\leftarrow}^{(2)} \\ &= -\frac{N'e}{h} \left[-\frac{1 + P_{FM}}{2} \int_{\mu}^{\mu_{\rightarrow}} T(\epsilon) d\epsilon + \frac{1 - P_{FM}}{2} \int_{\mu_{\leftarrow}}^{\mu} T(\epsilon) d\epsilon \right] \\ &\approx -\frac{N'e}{h} (-P_{FM} T|_{\epsilon=\mu}) \cdot \mu_s, \end{aligned} \quad (\text{S25a})$$

$$\begin{aligned} I_s^{(2)} &= I_{\rightarrow}^{(2)} - I_{\leftarrow}^{(2)} \\ &= -\frac{N'e}{h} \left[-\frac{1 + P_{FM}}{2} \int_{\mu}^{\mu_{\rightarrow}} T(\epsilon) d\epsilon - \frac{1 - P_{FM}}{2} \int_{\mu_{\leftarrow}}^{\mu} T(\epsilon) d\epsilon \right] \\ &\approx -\frac{N'e}{h} (-T|_{\epsilon=\mu}) \cdot \mu_s, \end{aligned} \quad (\text{S25b})$$

where the approximation is taken under the assumption that $\mu_s \ll \Delta\mu$, so that $T(\epsilon)$ is approximately a constant within the energy range from μ_{\leftarrow} to μ_{\rightarrow} , and thus they are evaluated at $\epsilon = \mu = -\Delta\mu/2$. The energy dependence of $I^{(2)}$ and $I_s^{(2)}$ follows that of $T(\epsilon)$ (Eqn. S20).

We can now rewrite Eqn. S23 and Eqn. S25 into matrix form

$$\begin{pmatrix} I \\ I_s \end{pmatrix} = -\frac{N'e}{h} \begin{pmatrix} \bar{T}|_{\mu}^{\mu_L} & -P_{FM}T|_{\epsilon=\mu} \\ P_{FM}\bar{T}|_{\mu}^{\mu_L} & -T|_{\epsilon=\mu} \end{pmatrix} \begin{pmatrix} \mu_L - \mu \\ \mu_s \end{pmatrix}, \quad (\text{S26})$$

which is Eqn. ?? in the main text. The different off-diagonal terms demonstrate the breaking of Onsager reciprocity in the nonlinear regime, since one of them depends on the integral of the transmission function, while the other depends on the transmission function itself. In the linear response regime ($\mu_L \approx \mu$), the two terms differ only by sign.

We write

$$\begin{pmatrix} I \\ I_s \end{pmatrix} = -\frac{1}{e} \begin{pmatrix} G_1 & G_2 \\ G_3 & G_4 \end{pmatrix} \begin{pmatrix} \mu_L - \mu \\ \mu_s \end{pmatrix}, \quad (\text{S27})$$

so that the matrix elements represent conductance, where $G_2 = (N'e^2/h) \cdot (-P_{FM}T|_{\epsilon=\mu})$ and $G_3 = (N'e^2/h) \cdot (P_{FM}\bar{T}|_{\mu}^{\mu_L})$. In Fig. S2, we plot G_2 and G_3 as a function of bias across the FMTJ ($(\mu_L - \mu)/e$) for $P_{FM} = -0.5$ and $N' = 1000$, values that are used to calculate the I - V curves in Fig. ??(d) (for other parameters see later in S.I.I).

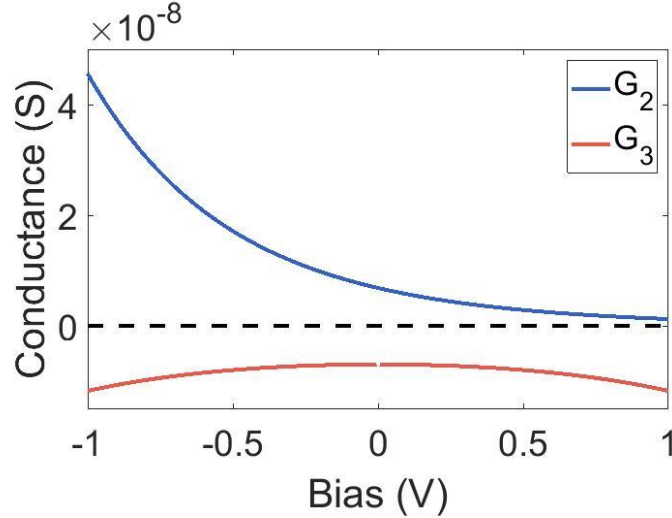


FIG. S2. Bias dependence of the off-diagonal elements of the conductance matrix describing tunneling through the FMTJ.

Note that $G_2 = -G_3$ at zero bias, as required by Onsager reciprocity in the linear response regime. The breaking of reciprocity in the nonlinear regime is exhibited by the unequal absolute values of G_2 and G_3 away from zero bias. Here G_2 increases monotonically with decreasing bias, while G_3 is symmetric in bias and is minimum at zero bias.

H. RECIPROCITY BREAKING BY THERMALLY ACTIVATED RESONANT TRANSMISSION THROUGH MOLECULAR ORBITALS

We discuss here the effect of the Fermi-Dirac distribution of electrons using resonant transmission through discrete molecular orbitals (levels), specifically the lowest-unoccupied molecular orbital (LUMO) and the highest-occupied molecular orbital (HOMO). This is illustrated in Fig. S3. We assume here the LUMO and HOMO levels are fixed at energies ϵ_{LU} and $-\epsilon_{HO}$ respectively ($\epsilon_{LU}, \epsilon_{HO} > 0$), with $\epsilon = 0$ defined as the average of the two (charge) electrochemical potentials on both sides of the molecule. The nonlinearity is now assumed to be fully due to the Fermi-Dirac distribution $F(\epsilon, \mu)$, which is different for the node and the electrode, and is also different for the two spin species in the node when a spin accumulation is considered.

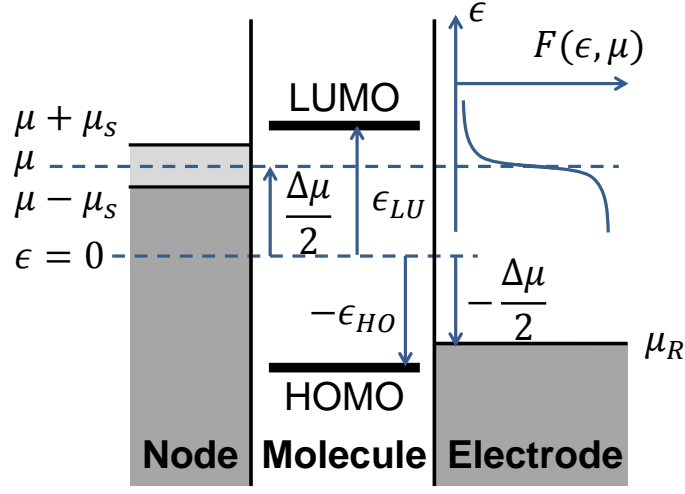


FIG. S3. Energy diagram of the electron transmission through molecular levels.

Consider the geometry in Fig. S3, at a given bias $\Delta\mu$ and a spin accumulation μ_s in the node, the spin-specific Fermi-Dirac functions for the two spin species in the node are

$$F_{L\rightarrow}(\epsilon, \Delta\mu, \mu_s) = \frac{1}{\exp\left(\frac{\epsilon - \Delta\mu/2 - \mu_s}{k_B T}\right) + 1}, \quad (\text{S28a})$$

$$F_{L\leftarrow}(\epsilon, \Delta\mu, \mu_s) = \frac{1}{\exp\left(\frac{\epsilon - \Delta\mu/2 + \mu_s}{k_B T}\right) + 1}, \quad (\text{S28b})$$

where we used subscript L to denote the node because its located on the left side of the molecule.

The Fermi-Dirac function in the node (neglecting the spin accumulation) and in the right electrode are

$$F_L(\epsilon, \Delta\mu) = \frac{1}{\exp\left(\frac{\epsilon - \Delta\mu/2}{k_B T}\right) + 1}, \quad (\text{S29a})$$

$$F_R(\epsilon, \Delta\mu) = \frac{1}{\exp\left(\frac{\epsilon + \Delta\mu/2}{k_B T}\right) + 1}. \quad (\text{S29b})$$

We model the resonant transmission through the molecular orbitals as energy-dependent transmission probability $t(\epsilon)$ that is only nonzero at the LUMO and the HOMO levels, which it is described by

$$t(\epsilon) = t_{LU}\delta(\epsilon - \epsilon_{LU}) + t_{HO}\delta(\epsilon + \epsilon_{HO}), \quad (\text{S30})$$

where t_{LU} and t_{HO} are the transmission probabilities through the LUMO and the HOMO, respectively, and $\delta(\epsilon)$ is a Dirac delta function.

An exact calculation should separately address the two spin orientations separately, but for our assumption of $\mu_s \ll \Delta\mu$, we will directly start from the linear-regime equation of coupled charge and spin transport (Eqn. S14)

$$\begin{pmatrix} I \\ -I_{sL} \end{pmatrix} = -\frac{Ne}{h} \begin{pmatrix} t & P_t t \\ P_t t & -(1 + 2P_t/\eta_r)t \end{pmatrix} \begin{pmatrix} \mu - \mu_R \\ \mu_s \end{pmatrix}. \quad (\text{S31})$$

This gives the charge current I

$$I = -\frac{Ne}{h} [t(\mu_L - \mu_R) + P_t t(\mu_{L\rightarrow} - \mu_{L\leftarrow})/2], \quad (\text{S32})$$

where we used $\mu_{L\rightarrow} = \mu + \mu_s$ and $\mu_{L\leftarrow} = \mu - \mu_s$.

At finite temperature, the two terms in the square bracket on the right-hand side of the equation should each be replaced by an energy-integral of the electron transmission function modified by the voltage- and temperature-dependent Fermi-Dirac distributions in both electrodes. We denote the two terms $I^{(1)}$ and $I^{(2)}$, and the first term

is

$$\begin{aligned}
I^{(1)} &= \int_{-\infty}^{\infty} t(\epsilon) [F_L(\epsilon, \Delta\mu) - F_R(\epsilon, \Delta\mu)] d\epsilon \\
&= t_{LU} [F_L(\epsilon_{LU}, \Delta\mu) - F_R(\epsilon_{LU}, \Delta\mu)] \\
&\quad + t_{HO} [F_L(-\epsilon_{HO}, \Delta\mu) - F_R(-\epsilon_{HO}, \Delta\mu)].
\end{aligned} \tag{S33}$$

We denote

$$\mathcal{F}_{\epsilon}(\Delta\mu) = \frac{1}{\Delta\mu} [F_L(\epsilon, \Delta\mu) - F_R(\epsilon, \Delta\mu)], \tag{S34}$$

to highlight the transmission at energy ϵ and under bias $\Delta\mu$. In this manner, we can write

$$I^{(1)} = [t_{LU} \mathcal{F}_{\epsilon_{LU}}(\Delta\mu) + t_{HO} \mathcal{F}_{-\epsilon_{HO}}(\Delta\mu)] \Delta\mu. \tag{S35}$$

Similarly, at finite temperature, the second term $I^{(2)}$ becomes

$$\begin{aligned}
I^{(2)} &= \frac{P_t}{2} (t_{LU} [F_{L\rightarrow}(\epsilon_{LU}, \Delta\mu, \mu_s) - F_{L\leftarrow}(\epsilon_{LU}, \Delta\mu, \mu_s)] \\
&\quad + t_{HO} [F_{L\rightarrow}(-\epsilon_{HO}, \Delta\mu, \mu_s) - F_{L\leftarrow}(-\epsilon_{HO}, \Delta\mu, \mu_s)]).
\end{aligned} \tag{S36}$$

We define

$$\begin{aligned}
&\mathcal{F}'_{L,\epsilon}(\Delta\mu) \\
&= \frac{1}{2\mu_s} [F_{L\rightarrow}(\epsilon, \Delta\mu, \mu_s) - F_{L\leftarrow}(\epsilon, \Delta\mu, \mu_s)] \\
&\approx \frac{\partial[F_L(\epsilon, \Delta\mu)]}{\partial\Delta\mu},
\end{aligned} \tag{S37}$$

where the approximation is taken under the assumption of $\mu_s \ll \Delta\mu$.

With this, we have

$$I^{(2)} = P_t [t_{LU} \mathcal{F}'_{L,\epsilon_{LU}}(\Delta\mu) + t_{HO} \mathcal{F}'_{L,-\epsilon_{HO}}(\Delta\mu)] \mu_s. \tag{S38}$$

Similarly, the expression of $-I_{sL}$ at finite temperature can also be derived from the linear regime expression. The nonlinear coupled spin and charge transport equation, due to the thermally activated resonant transmission via the LUMO and the HOMO levels, is therefore

$$\begin{pmatrix} I \\ -I_{sL} \end{pmatrix} = -\frac{Ne}{h} \begin{pmatrix} t_{LU} \mathcal{F}_{\epsilon_{LU}}(\Delta\mu) + t_{HO} \mathcal{F}_{-\epsilon_{HO}}(\Delta\mu) & P_t [t_{LU} \mathcal{F}'_{L,\epsilon_{LU}}(\Delta\mu) + t_{HO} \mathcal{F}'_{L,-\epsilon_{HO}}(\Delta\mu)] \\ P_t [t_{LU} \mathcal{F}_{\epsilon_{LU}}(\Delta\mu) + t_{HO} \mathcal{F}_{-\epsilon_{HO}}(\Delta\mu)] & -(1 + 2P_t/\eta_r) [t_{LU} \mathcal{F}'_{L,\epsilon_{LU}}(\Delta\mu) + t_{HO} \mathcal{F}'_{L,-\epsilon_{HO}}(\Delta\mu)] \end{pmatrix} \begin{pmatrix} \mu - \mu_R \\ \mu_s \end{pmatrix}, \tag{S39}$$

where we have assumed P_t, η_r do not depend on energy.

The breaking of reciprocity arises from the different forms of the off-diagonal terms of the transport matrix. While the bottom-left term scales with the electron occupation function, the top-right terms scales with its derivative. In the linear response regime, the two terms are equal and Onsager reciprocity is present.

If required, this nonlinear form can be easily extended to the 3×3 matrix for a generalized situation considering also a spin accumulation μ_{sR} on the right-hand side of the molecule. Then the third column will be modified similarly to the second column using the derivative of the electron occupation function in the right electrode $F_R(\epsilon, \Delta\mu)$.

Similar to the FMTJ, we can write the above equation into

$$\begin{pmatrix} I \\ -I_s \end{pmatrix} = -\frac{1}{e} \begin{pmatrix} g_1 & g_2 \\ g_3 & g_4 \end{pmatrix} \begin{pmatrix} \mu - \mu_R \\ \mu_s \end{pmatrix}, \tag{S40}$$

where the matrix elements represent conductances. We plot the off-diagonal terms as a function of bias $((\mu - \mu_R)/e)$ for transmission only through the LUMO level ($t_{LU} = 1, t_{HO} = 0, \epsilon_{LU} = 0.6$ eV) for $P_t = 0.85$ and $N = 1000$, as shown in Fig. S4.

Note that $g_2 = g_3$ at zero bias, as required by Onsager reciprocity in the linear response regime. The reciprocity is broken as bias shifts away from zero, and the two conductances are no longer equal. Here g_2 increases monotonically with bias, while g_3 is bias-symmetric and reaches minimum at zero bias.

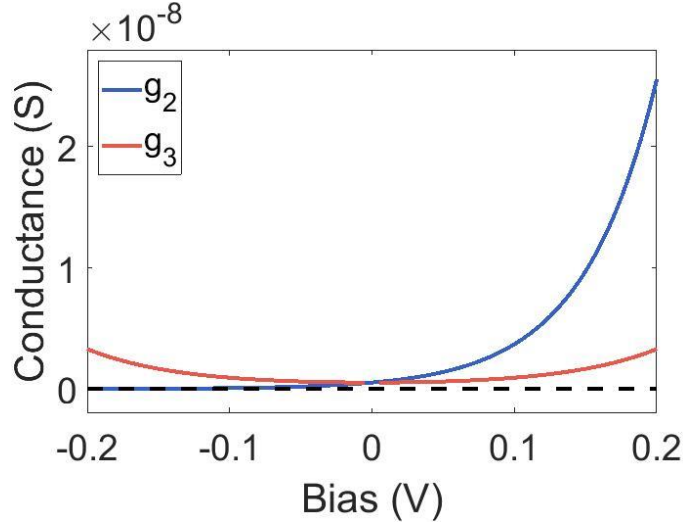


FIG. S4. Bias dependence of the off-diagonal elements of the conductance matrix describing thermally activated conduction through the LUMO.

I. PARAMETERS FOR EXAMPLE I - V CURVES

(1) For calculating the I - V curves in Fig. ??(d) we have used the following parameters: Energy dependent FM tunnel transmission $T(\epsilon)$ for a tunnel barrier with height $\Phi = 2.1$ eV, and width $w = 1.0$ nm. The number of channels are set as $N' = 1000$ and $N = 5000$, the values are chosen taking into account the device length scale. For example, if using Ni as FM, when assuming each atom provides one channel, $N' = 1000$ corresponds to roughly an area of 100 nm^2 . The transmission through the chiral component is set linear and uses the same transmission value as the FM tunnel barrier at zero bias. The polarization values are $P_{FM} = \pm 0.5$, $P_t = 0.85$, and the quantity η_r is set as $\eta_r = 0.9$. The same parameters are used to obtain the conductances in Fig. S2.

(2) For calculating the I - V curves in Fig. ??(b-c) we have used the following parameters: Temperature at 300 K, the LUMO level at $\epsilon_{LU} = 0.6$ eV, and the HOMO level at $-\epsilon_{HO} = -0.6$ eV. For Fig. ??(b), the LUMO transmission $t_{LU} = 1$ and the HOMO transmission $t_{HO} = 0$, while for Fig. ??(c) the two values are interchanged. The number of channels are set as $N' = 1000$ and $N = 200$. The transmission through the FM tunnel barrier is set linear and uses the same transmission value as the FM tunnel barrier in case (1) at zero bias. The polarization values are $P_{FM} = \pm 0.5$, $P_t = 0.85$, and the quantity η_r is set as $\eta_r = 0.9$. The same parameters are used to obtain the conductances in Fig. S4.

(3) For the chiral spin valve in Fig. ??(f), we use the same tunnel transmission function and the same barrier parameters as in case (1) for both chiral components (both nonlinear), and do not consider the thermally activated molecular level transmission. The number of channels are set as $N' = 1000$ and $N = 20000$. The first chiral component has polarization ± 0.5 , and the second one 0.85, both have $\eta_r = 0.9$.

(d) For the example in Fig. ??(g), the tunnel barrier uses the same parameters as the FMTJ in case (1), but has zero polarization. The chiral component transmission is set linear and uses the same set of parameters as in case (1). The dashed curve is obtained by forcing $\mu_s = 0$ for all bias values.

J. SIGN OF THE NONLINEAR 2T MR

We summarize here, separately for the two nonlinear mechanisms, how the sign of the MR depends on the chirality, the charge carrier type, and the bias direction. First of all, we define the MR for the device in Fig. ??(a) following

$$MR = \frac{I_+ - I_-}{I_+ + I_-} \times 100\%, \quad (\text{S41})$$

where I_+ represents the charge current measured with the FM polarization $P_{FM} > 0$, which corresponds to a spin-right polarization of the injected electrons, and I_- corresponds to the current measured when the FM generates a spin-left polarization.

For the bias direction, we describe it in terms of electron movement direction (opposite to charge current) with respect to the circuit components. For example, in Fig. ??(a), the positive bias voltage corresponds to an electron movement from the chiral component (CC) to the FMTJ.

For the (sign of) chirality, we label it as D and L. Here we (arbitrarily) assume that a D-chiral component favors the transmission of electrons with spins parallel to the electron momentum, while a L-chiral component favors the anti-parallel. The exact correspondence between the chirality and the favored spin orientation depends on the microscopic details of the spin orbit interaction.

According to these definitions, the sign of the MR is summarized in the following tables.

TABLE SI. Summary of the sign of MR for nonlinear tunneling through FMTJ

chirality	electron direction	carrier type	MR
D	CC to FMTJ	electron	+
L	CC to FMTJ	electron	-
D	FMTJ to CC	electron	-
L	FMTJ to CC	electron	+

TABLE SII. Summary of the sign of MR for nonlinear transmission through molecular orbitals

chirality	electron direction	carrier type	MR
D	CC to FMTJ	electron	+
L	CC to FMTJ	electron	-
D	FMTJ to CC	electron	-
L	FMTJ to CC	electron	+
D	CC to FMTJ	hole	-
L	CC to FMTJ	hole	+
D	FMTJ to CC	hole	+
L	FMTJ to CC	hole	-

* xu.yang@rug.nl

[S1] Laurence D Barron, “True and false chirality and absolute asymmetric synthesis,” *Journal of the American Chemical Society* **108**, 5539–5542 (1986).

[S2] L D Barron, “Reactions of chiral molecules in the presence of a time-non-invariant enantiomorphous influence: a new kinetic principle based on the breakdown of microscopic reversibility,” *Chemical Physics Letters* **135**, 1–8 (1987).

[S3] N Micali, H Engelkamp, P G van Rhee, P C M Christianen, L Monsù Scolaro, and J C Maan, “Selection of supramolecular chirality by application of rotational and magnetic forces,” *Nature Chemistry* **4**, 201 (2012).

[S4] Koyel Banerjee-Ghosh, Oren Ben Dor, Francesco Tassinari, Eyal Capua, Shira Yochelis, Amir Capua, See-Hun Yang, Stuart SP Parkin, Soumyajit Sarkar, Leeor Kronik, *et al.*, “Separation of enantiomers by their enantiospecific interaction with achiral magnetic substrates,” *Science* **360**, 1331–1334 (2018).

[S5] Arne Brataas, Yu V Nazarov, and Gerrit E W Bauer, “Finite-element theory of transport in ferromagnet–normal metal systems,” *Physical Review Letters* **84**, 2481 (2000).

[S6] Jens H Bardarson, “A proof of the Kramers degeneracy of transmission eigenvalues from antisymmetry of the scattering matrix,” *Journal of Physics A: Mathematical and Theoretical* **41**, 405203 (2008).

[S7] Shlomi Matityahu, Yasuhiro Utsumi, Amnon Aharony, Ora Entin-Wohlman, and Carlos A Balseiro, “Spin-dependent transport through a chiral molecule in the presence of spin-orbit interaction and nonunitary effects,” *Physical Review B* **93**, 075407 (2016).

[S8] Xu Yang, Caspar H van der Wal, and Bart J van Wees, “Spin-dependent electron transmission model for chiral molecules in mesoscopic devices,” *Physical Review B* **99**, 024418 (2019).

[S9] Lars Onsager, “Reciprocal relations in irreversible processes. II,” *Physical Review* **38**, 2265 (1931).

[S10] R Jansen, A Spiesser, H Saito, Y Fujita, S Yamada, K Hamaya, and S Yuasa, “Nonlinear electrical spin conversion in a biased ferromagnetic tunnel contact,” *Physical Review Applied* **10**, 064050 (2018).